Unimolecular Reaction Dynamics of CH_3COCl and FCH_2COCl: An Infrared Chemiluminescence and ab Initio Study

A. Srivatsava and E. Arunan*

Department of Chemistry, Indian Institute of Technology, Kanpur 208 016, India

G. Manke II and D. W. Setser

Department of Chemistry, Kansas State University, Manhattan, Kansas 66506

R. Sumathi†

Lehrstuhl fur Theroetische Chemie, Universtat Bonn, Wegelerstrasse 12, 53115 Bonn, Germany

Received: December 4, 1997; In Final Form: May 13, 1998

The F + CH_3COCl and H + ICH_2COCl reaction systems were studied by the infrared chemiluminescence method in a flow reactor. The primary reaction of F + CH_3COCl gives a nascent HF(v) distribution of P_1-P_3 = 21:52:27. A linear surprisal analysis gives P_0 = 3 and $\langle f_v(HF)\rangle$ = 0.60, which is typical for H abstraction reactions by F atoms. The C−H bond energy in acetyl chloride is estimated as ≤101.2 kcal mol^{-1}, from the highest HF(v, J) level populated in the primary reaction. The H + ICH_2COCl primary reaction leads to HI + CH_2COCl. The secondary F + CH_2COCl and H + CH_2COCl reactions give chemically activated FCH_2COCl*/CH_3COCl* molecules. The 1,2-HCl elimination channel is the dominant unimolecular pathway for both reactions under our experimental conditions. The HCl(v) distribution from CH_3COCl* is P_1-P_4 = 39:32:20:9. Surprisal analysis was used to estimate the P_0 value as 36% and $\langle f_v(HCl)\rangle$ = 0.12. The reaction time had to be increased from ≤0.2 ms to ≥0.5 ms to record the HCl(v) emission from F + CH_2COCl, and the best distribution was P_1-P_4 = 68:24:5:3. The estimated $\langle f_v(HCl)\rangle$ was only 0.06 which is a lower limit due to HCl(v) relaxation. The CO($v = 1 \rightarrow 0$) emission could also be observed from this reaction with an intensity that was typically less than 10% of the HCl(v) emission. Ab initio calculations for FCH_2COCl at MP2/6-31G* level give the threshold energy for HCl elimination as 61 kcal mol^{-1}, which is 12 kcal mol^{-1} larger than that for CH_3COCl at the same level. The threshold energies for the other reactions of FCH_2COCl are 81.0 for CO elimination, 82.5 for C−C dissociation, and 78.4 for C−Cl dissociation. RRKM and ab initio calculations indicate that CO formation results from the $FCH_2COCl \rightarrow FCH_2 + COCl$ dissociation step followed by $COCl \rightarrow CO + Cl$. For CH_3COCl*, with 105 kcal mol^{-1} energy, HCl elimination accounts for 98% of the total reaction and C−C dissociation accounts for the rest. The C−Cl dissociation channel is not important for either molecule at these energies.

I. Introduction

The four-centered elimination of HX from haloethanes has become a textbook example for unimolecular reactions although some details of the structure of the transition state (TS) are still debated.[1] The TS is nearly planar and the experimental activation energies are 55−70 kcal mol^{-1} for various molecules. The HX elimination channel is the dominant reaction pathway for activated molecules at energies below 100 kcal mol^{-1} as the dissociation channels have large energy barriers. Numerous studies on the dynamics of these reactions, both experimental[2−6] and theoretical,[7−9] have been made for haloethanes. For acetyl halides, the activation energy may be lower than that of haloethanes as one of the C atoms already has sp^2 hybridization. In fact, Sumathi and Chandra[10] have calculated a barrier of 48 kcal mol^{-1} for HCl elimination from CH_3COCl, which is 8 kcal mol^{-1} lower than that for CH_3CH_2Cl.[1] However, experimental investigations of the unimolecular HX elimination from CH_3COCl have not been reported to the best of our knowledge. In the present study, we identify the existence of the unimolecular HCl elimination channel from CH_3COCl and FCH_2COCl by observing HCl formation from infrared chemiluminescence (IRCL).

The Kansas State laboratory has been using IRCL from a fast flow reactor to study the dynamics of chemical reactions.[5,11−14] These studies include the HX elimination from haloethanes[5] and H_2O elimination from CH_3CH_2OH[13] and CH_3COOH.[14] For all HX elimination cases, the vibrational distribution of HX (X = halogen or OH) monotonically declines with increasing E_v(HX), and the fraction of available energy appearing as HX vibration, $<f_v(HX)>$, is 0.1−0.2. Considering the similarity in the dynamics of H_2O elimination from CH_3CH_2OH and CH_3COOH, we expect that HCl elimination from CH_3-

* Corresponding author. Currently at the Department of Inorganic and Physical Chemistry, Indian Institute of Science, Bangalore-560 012, India.
† On leave from Manonmaniam Sundaranar University, Tirunelveli-627 002, India.

S1089-5639(98)00415-0 CCC: $15.00 © 1998 American Chemical Society
Published on Web 07/17/1998

COCl would resemble that of haloethanes. Recently, Harmony and co-workers[15] have used thermal decomposition of haloacetyl halides ($ClCH_2COCl$ and $BrCH_2COBr$) as a precursor reaction to study the spectroscopy of HCCl and HCBr as follows:

$$XCH_2COX \rightarrow XHC{=}C{=}O + HX \quad \text{(R1)}$$

$$XHC{=}C{=}O \rightarrow XCH + CO \quad \text{(R2)}$$

Their experiment clearly suggests that the HX elimination is a dominant channel for haloacetyl halide decomposition. The IRCL studies on such reactions could complement the work on HX elimination from haloethanes and could contribute to our understanding on the transition states for four-center elimination reactions.

The following reaction schemes were chosen to study CH_3COCl and FCH_2COCl:

$$F + CH_3COCl \rightarrow HF(v) + CH_2COCl \quad \text{(R3)}$$

$$F + CH_2COCl \rightarrow FCH_2COCl^* \quad \text{(R4)}$$

$$H + ICH_2COCl \rightarrow HI + CH_2COCl \quad \text{(R5)}$$

$$H + CH_2COCl \rightarrow CH_3COCl^* \quad \text{(R6)}$$

The chemically activated FCH_2COCl^*/CH_3COCl^* can have various reaction pathways, and from the ab initio results for CH_3COCl[10] we believe that HCl elimination will be the dominant pathway:

$$FCH_2COCl^* \rightarrow HCl(v) + FCHCO \quad \text{(R7)}$$

$$CH_3COCl^* \rightarrow HCl(v) + CH_2CO \quad \text{(R8)}$$

The other pathways are considered in the later sections. Reaction R3 has not been reported previously, but it should be very similar to the other F + HR reactions, where HR is a polyatomic organic molecule.[11] These bimolecular H abstraction reactions give an inverted HF(v) distribution with $\langle f_v \rangle$ of 0.5−0.6. Reactions R4 and R6 could occur by direct abstraction as well, leading to HF and HCl, respectively. However, our experiments suggest that abstraction is not important for reaction R6. For reaction R4, it will be difficult in our experiments to observe direct H abstraction due to the strong HF(v) emission from the primary step (reaction R3).

The threshold energy for reaction R7 and enthalpies of formation of some of the species are not available at present. We have performed quantum chemical calculations at correlated levels (MP2/6-31G*//MP2/6-31G*) to estimate the threshold energies and enthalpy changes for all the reaction pathways from FCH_2COCl. We have also analyzed the potential energy surface of FCH_2COCl and identified the transition states for various molecular decomposition channels. For CH_3COCl, similar results are already available,[10] but at the MP2/6-31G*//HF/6-31G* level. Toto et al.[1] noted that adding correlation affects the TS geometry more significantly for the HCl elimination than for HF elimination from the haloethanes. We have now optimized the geometry at the MP2/6-31G* level and also obtained the frequencies for the molecule and the TS at this level. We have further extended the calculations to MP2/6-311++G** for this reaction, R8, to look at the effect of basis set size beyond 6-31G*. TST and RRKM calculations have been carried out to determine the importance of different channels for the chemically activated CH_3COCl/FCH_2COCl.

II. Experiment

The experimental method has been previously described in detail, and we give only a brief summary of the operation of the flow reactor, which used Ar as the carrier gas.[5] The H/F atoms, produced in a microwave discharge of 10% H_2/CF_4 in Ar, were added at the front end of the flow reactor. The reagent ICH_2COCl/CH_3COCl was added 20 cm downstream, just before the observation zone, which was viewed through a NaCl window. For ICH_2COCl, Ar was passed over the solid sample at room temperature and the concentration was found by the weight loss. Infrared emission spectra were recorded with a resolution of 1−2 cm^{-1} by a Bio-Rad spectrometer (FTS-60) with InSb detector, cooled to liquid N_2 temperature. Reactions R3, R5, and R8 could be studied at 0.5 Torr with the maximum pumping speed, which corresponds to a flow velocity of 120 m s^{-1} and an observation time of 0.2 ms. Under such conditions the HX(v) distribution observed is nascent.[5,11,12] The rotational distributions are 300 K Boltzmann except for a remnant of the original distribution for HF(v, $J > 8$). The HI emission could not be observed from reaction R5 because of its very small Einstein coefficient for emission. To observe the HCl(v) emission from the secondary reaction R7, the observation time had to be increased to ≥0.5 ms. The experimental conditions were varied to determine the extent of HX(v) relaxation for longer observation time. In experiments that showed HCl emission from FCH_2COCl^*, weak CO(1 → 0) emission could also be observed. The source of CO emission is discussed in the following sections.

The peak heights of the resolved vibrational−rotational lines of HF/HCl were converted to populations by dividing them by the respective Einstein coefficients[16] and the instrumental response function. For HF(v, $J \leq 8$) levels and HCl, dividing the rotational populations by the Boltzmann factor directly gives the vibrational population. The HF(v, $J \leq 8$) level populations, if present, were then added to get the total population in each vibrational level. The rotational structure of the CO emission was not resolved, and the total area was divided by the Einstein coefficient (35.8 s^{-1})[17] and the response function to estimate the relative CO concentration.

III. Results and Discussion

a. Thermochemistry. The available energy, E_{av}, for the products from any chemical reaction is calculated as follows[11]

$$E_{av} = -\Delta H^\circ(0\ \text{K}) + E_a + E_{th} \quad (1)$$

where the first term is the enthalpy of the reaction at 0 K. The activation energy, E_a, for H abstraction reactions by F is generally very small and is taken as 1 kcal mol^{-1}. For reaction R3, the thermal energy, E_{th}, is taken as $3RT$ assuming that the polyatomic thermal vibrational energy is unavailable to the HF product. For the addition−elimination reactions, R4 and R6−R13, the vibrational energy of the radical (≈1.3 kcal mol^{-1} at 300 K) is included in E_{th}. The sum of E_a and E_{th} gives the energy of reactive collisions according to Tolman's definition of activation energy.[11] For the primary reaction R3, the ΔH° is the difference in bond energies between the F−H bond in HF and the C−H bond in CH_3COCl. The D_0(C−H) is not available for CH_3COCl. However, these H atom abstraction reactions lead to HF(v, J) levels that extend to the thermo-

chemical limit.[11] The highest populated HF(v, J) level from reaction R3 is $v = 3$, $J = 8$, and its energy is 12 681 cm^{-1} or 36.2 kcal mol^{-1}. The HF($v = 3$, $J = 9$) level is at 37.1 kcal mol^{-1}, and we took E_{av} as 37 kcal mol^{-1}. With these data, we estimate the $\Delta H°_f$(CH_2COCl, 0 K) as ≤ -6.3 kcal mol^{-1} and the C−H bond energy in CH_3COCl as ≤ 101.2 kcal mol^{-1}, which seems reasonable. The C−H bond energies in H−CH_2-CH_3 and H−CH_2COCH_3 are virtually identical (98 kcal mol^{-1}), and our estimate for H−CH_2COCl is close to that of H−CH_2-Cl (100.9 kcal mol^{-1}).[18] We take the C−H bond energy in CH_3COCl as 101 kcal mol^{-1}. The $\Delta H°_f$ (in kcal mol^{-1}) at 0 K for F (18.5 ± 0.1) and HF (−65.1 ± 0.2)[19] and CH_3COCl (−55.9 ± 0.2)[20] were taken from the literature.

From the above estimate of C−H bond energy in CH_3COCl, E_{av} for reactions R6 and R8 can be calculated, and they are 105 and 85 kcal mol^{-1}, respectively. To the best of our knowledge, experimental or theoretical data are not available for the $\Delta H°_f$ for FCH_2COCl. Hence, the $\Delta H°$ had to be estimated for reactions R4 and R7. Primary C−F bond energies are of the order of 110 kcal mol^{-1}; e.g., CH_3F (110) and C_2H_5F (108),[18] and CH_2ClF (108).[5] We used a C−F bond energy of 108 kcal mol^{-1} to estimate the $\Delta H°_f$ for FCH_2COCl as −95.8 kcal mol^{-1} at 0 K. The chemically activated CH_3COCl/FCH_2-$COCl$ molecules produced in R6/R4, can react by several molecular elimination and bond dissociation pathways. Reaction pathways for CH_3COCl have been considered in ref 10. The C−F bond is expected to be stronger than any other single bond in FCH_2COCl, and so all the single-bond dissociation processes are energetically accessible. The reactions involved are given below. Estimated $\Delta H°$ in kcal mol^{-1} is given for each reaction in parentheses.

$$FCH_2COCl \rightarrow HCl(v) + CHFCO \quad (39) \qquad \text{(R7)}$$

$$\rightarrow FCl + CH_2CO \quad (70) \qquad \text{(R9)}$$

$$\rightarrow CH_2FCl + CO \quad (8) \qquad \text{(R10)}$$

$$\rightarrow CH_2FCO + Cl \quad (83) \qquad \text{(R11)}$$

$$\rightarrow CH_2F + COCl \quad (83) \qquad \text{(R12)}$$

$$\rightarrow HCCOCl + HF \quad (?) \qquad \text{(R13)}$$

Some tertiary reactions are possible as given below:

$$COCl \rightarrow CO + Cl \quad (7) \qquad \text{(R14)}$$

$$CHFCO \rightarrow CHF + CO \quad (42) \qquad \text{(R15)}$$

$$CH_2FCO \rightarrow CH_2F + CO \quad (7) \qquad \text{(R16)}$$

The following $\Delta H°_f$ values from the literature were used in the above estimates. Experimental values (in kcal mol^{-1}) are available for Cl (28.6 ± 0.0), HCl (−22.0 ± 0.0), FCl (−12.0 ± 0.0), CO (−27.2 ± 0.0), and CH_2FCl (−60.8 ± 3.1);[19] COCl (−5.6 ± 0.7);[21] CH_2CO (−14.0 ± 0.6);[22] and CH_2F (−7 ± 1).[18] For CHF, the experimental $\Delta H°_f$(298 K) varies from 26[23] to 39,[24] and we have used the theoretical estimate (33.9) of Rodriquez and Hopkinson[25] with an estimated uncertainty of 2.4 kcal mol^{-1}. For FCHCO and FCH_2CO, experimental data are not available at present, and $\Delta H°_f$(298 K) for FCHCO (−35.2) and FCH_2CO (−41.2) were taken from the recent, extensive theoretical work of Zachariah and co-workers.[26] These authors calculate $\Delta H°_f$(CHF, 298 K) to be 31.5 in close agreement with the value we use. However, for several of the oxyfluoro species, a significant difference ($\geq$3.6 kcal mol^{-1}) exists between the calculated and experimental values. In view of this, the $\Delta H°_f$ values for these species were used as such without thermal corrections. For the same reason, the uncertainty in $\Delta H°$ above are not listed, and it could be large, 5 kcal mol^{-1} or more. We have also carried out ab initio calculations to estimate the enthalpies and threshold energies for all these reactions, the details of which are given in section IV.

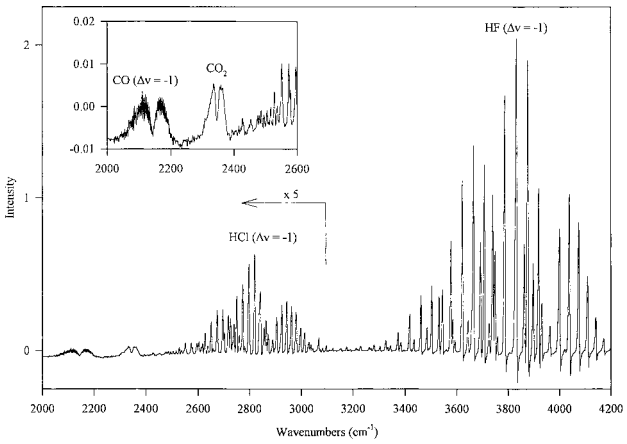

Figure 1. The infrared chemiluminescence spectra of HF(v), HCl(v), and CO(v) from the F + CH_3COCl reaction system for [F] = 1.44 × 10^{13}, [CH_3COCl] = 5.88 × 10^{13}, both in molecules cm^{-3}, Ar pressure = 2.0 Torr, and an observation time = 0.92 ms.

TABLE 1: HF(v) Distribution from Some F + CH_3X Reactions[a]

X	E_{av}	P_0	P_1	P_2	P_3	$-\lambda_v$	$\langle f_v \rangle$
COCl	37		21	52	27		
		3	20	50	27	9.8 ± 0.6	0.60
Cl	39		9	36	55	11.2 ± 0.6	0.68
		1	9	36	54		
CH_3	41		12	52	36	9.3 ± 0.8	0.58
		2	12	51	35		
OCH_3	45		26	48	26	6.2 ± 0.6	0.43
		12	23	42	23		

[a] First line gives the experimental distribution, and the second line gives the results of surprisal analysis using model 2 prior which includes polyatomic rotations in the surprisal calculations. CH_3COCl results are from this work, and other results are from ref 11. The uncertainty in the populations given for CH_3COCl is 2, i.e., $P_1 = 21 \pm 2$, $P_2 = 52 \pm 2$, and $P_3 = 27 \pm 2$ from six different experiments. E_{av} is the available energy (kcal mol^{-1}) for the products, and $\langle f_v \rangle$ is the fraction of it that goes into HF vibration.

b. HF(v) Distribution from the Primary Reaction (R3). Figure 1 shows the HF(v), HCl(v), and CO(v) emission spectra from the F + CH_3COCl system. The apparent CO_2 emission is from the background subtraction and has no significance, i.e., it is the consequence of incomplete removal of CO_2 absorption by the flushing. The HF(v) distribution did not vary with [F] or [CH_3COCl] for an observation time below 0.2 ms and for concentration range 1−5 × 10^{12} molecules cm^{-3}. The average distribution from six different experiments is HF($v = 1-3$) = 21:52:27. The distribution is strongly inverted as is true for most H atom abstraction reactions by F. The population in $v = 0$ level was estimated using surprisal analysis.[11] The surprisal plot was linear and λ_v and P_0 depended on the prior model used. Results from model 2 prior[11] (correlation coefficient = 0.998), which includes rotations of the polyatomic product (CH_2COCl in this case), are $\lambda_v = -9.8 \pm 0.6$, $\langle f_v(HF) \rangle = 0.6$, and P_0−P_3 = 3:20:50:27. Table 1 compares the vibrational distributions and surprisal results for several F + HR reactions. The results from CH_3COCl are very similar to those for CH_3Cl and C_2H_6.

TABLE 2: Relative Population in HF(v, $J > 8$) Compared to the Total HF(v) Population from Some Experiments for $v = 1$ and 2 from the F + CH_3COCl Reaction System[a]

no.	[F]	[R]	P	Δt	$v = 1$	$v = 2$
1	1.6	3.6	0.43	0.20	10.6	2.0
2	2.8	5.9	0.44	0.20	6.4	1.8
3	2.0	5.6	0.60	0.28	3.6	1.4
4	14.4	39.0	1.00	0.46	15.1	9.7
5	14.4	55.8	2.00	0.92	12.6	12.9

[a] [F] and [R] give the concentration of the F atoms and reagent in 10^{12} molecules cm^{-3}, P = pressure in Torr, and Δt = time in ms, the last two columns give the percentage of HF(v) population in the $J > 8$ levels. The HF($v = 1-3$) distribution in experiments 2−5 were 25:52:23, 26:53:21, 53:37:10, and 68:26:6, respectively. These were not used in determining the nascent distribution given in Table 1. For comparison, experiment 1 gave 19:53:28.

This comparison clearly suggests that the HF(v) distribution obtained is nascent.

c. HF(v) Rotational Distribution from Primary Reaction (R3). The HF(v, $J > 8$) levels do not entirely equilibrate under our experimental conditions, and this fact has been used to estimate the HF rotational energy distribution in several reactions.[5] Some of the experiments resulted in emission from HF(v, $J > 8$) levels, though the emission was weak. Table 2 shows the relative population of HF($J > 8$) to the total population in the $v = 1$ and 2 levels. For the conditions that gave nascent vibrational distribution (entry 1 in Table 2), the HF($J > 8$) population was 10.6 and 2.0% for the $v = 1$ and $v = 2$ levels, respectively. Clearly, the HF rotational excitation from the primary reaction is rather modest. Several experiments were done for longer observation time to observe HCl emission from reaction R7, and the HF(v) rotational distributions showed some interesting trends which are discussed below.

Comparing experiments 1 and 2 in Table 2, the high J population has decreased from 10.6% to 6.4%, and it is most likely the result of rotational relaxation by [R], i.e., [CH_3COCl]. The observation time is the same for both experiments. From results of experiment 3, it is clear that increasing $P\Delta t$ (P is the Ar pressure and Δt is the observation time) also causes rotational relaxation, which has been observed earlier.[5] However, for experiments 4 and 5 which correspond to longer observation time (0.5 to 1 ms), the P, [R], and [F] have increased and the high J population for $v = 1$ and 2 have *increased* to 15 and 10%. Under these conditions, the HF(v) distribution had dramatically changed from the nascent 21:52:27 to 53:37:10 for experiment 4. This could be due to two factors. The vibrational relaxation of HF could proceed through v → R (vibrational to rotational) mechanism, wherein the HF(v, low J) goes to HF($v - 1$, high J) in collisions with CH_3COCl/F/Ar. Such v → R transfer has been observed in several cases.[27] The other possibility is that 1,1-HF elimination from FCH_2COCl* is taking place which could contribute to an increase in HF($v = 1$ and 2) as well as the high J population.[5] However, results from our ab initio calculations rule out the importance of HF elimination from FCH_2COCl for energies below 115 kcal mol^{-1}, vide infra.

d. HCl(v) Distribution from the Secondary Reactions R7 and R8. Reaction R8 could be observed under conditions that gave a nascent distribution, and hence it is discussed first. The HCl(v) rotational distributions are Boltzmann, and the vibrational populations were directly determined as described above. Table 3 lists the HCl(v) distribution from both reactions. The distribution, as expected for a unimolecular elimination reaction, is monotonically declining. The HCl(v) distribution obtained from CH_3COCl* in three different experiments were somewhat different, and we take the experiment 1 distribution as nascent and it is P_1-P_4 = 39:32:20:9. The signal-to-noise ratio for the $v = 4$ emission was poor, and experiment 1 gave the best spectrum. Also, model 3 surprisal analysis, which includes all the degrees of freedom for the polyatomic product, gave a linear surprisal plot with a correlation coefficient of 0.994 for this distribution. The P_0 was estimated as 36%, and $\langle f_v(HCl)\rangle$ was 0.12. Table 4 compares the HX(v) distribution from haloethanes with CH_3COCl, and the results show striking similarity. This and the sum rule analysis discussed later in this section convince us that the HCl(v) distribution reported in Table 4, entry 1, for CH_3COCl is nascent.

TABLE 3: HCl(v) Distribution from H + CH_2COCl and F + CH_2COCl Reactions[a]

no.	[F]/[H]	[R]	P	Δt	P_1	P_2	P_3	P_4
1	13.0	10.0	0.45	0.17	39.1	31.9	19.6	9.4
2	6.6	16.0	0.45	0.17	49.6	30.6	19.8	
3	13.0	16.0	0.45	0.17	46.9	32.4	14.8	5.9
4	14.4	39.1	1.00	0.46	67.4	24.2	5.3	3.1
5	10.1	19.2	2.00	0.65	70.0	23.4	6.6	trace
6	14.4	55.8	2.00	0.92	77.6	18.3	2.9	1.1
7	14.4	65.1	2.00	0.92	79.2	18.0	2.3	0.5

[a] Experiments 1−3 are for H + CH_2COCl and 4−7 are for F + CH_2COCl. The column titles have the same meaning as in Table 2. The HF($v = 1-3$) distribution from experiments 4−7 are 53:37:10, 63:30:7, 68:26:6, and 68:26:6, respectively.

TABLE 4: HX(v) Distribution from Some Elimination Reactions[a]

molecule	P_0	P_1	P_2	P_3	P_4	$-\lambda_v$	$\langle f_v\rangle$
CH_3COCl		39.0	31.9	19.6	9.4		
	36.4	24.9	20.3	12.4	6.0	7.4	0.12
FCH_2COCl		67.4	24.2	5.3	3.1		
	66.9	22.3	8.0	1.8	1.0	*b*	0.06
CH_3CH_2Cl[6]		39.0	29.0	22.0	10.0		
	29.9	22.3	20.3	15.4	7.1	10.1	0.18
CH_3CH_2F[5]		41.1	31.1	18.9	6.9[c]		
	37.2	25.6	19.4	11.8	4.3	10.1	0.15
CF_3CH_3[5]		53.0	32.0	12.0	3.0		
	43.0	30.2	18.2	6.8	1.7	10.5	0.13

[a] First line gives the experimental distribution, and the second line gives the results from surprisal analysis. The superscripts in the molecules give the reference number for the data, and CH_3COCl and FCH_2COCl are from this work. [b] For FCH_2COCl, the surprisal plot was not linear and the P_0 was estimated as 3 times the P_1. Also, the $\langle f_v\rangle$ given here should be taken as a lower limit. By using the sum rule and results from CH_3COCl, we estimate the $\langle f_v\rangle$ for this reaction to be 0.11. See text. [c] This reaction also gives $v = 5$ with $P_5 = 2.0$; after renormalization, $P_5 = 1.7$.

The HCl(v) emission could not be observed from reaction R7 for observation time ≤0.2 ms and it was observed for longer observation time (≥0.5 ms) only. Table 3 lists the HCl(v) distribution from FCH_2COCl* in four experiments. The HCl(v) distribution shows relaxation as the Δt and [R] increase. For the conditions used in all these experiments, the HF(v) distribution from primary reaction R3 was also affected by relaxation, and the HCl(v) distribution is not nascent. We choose the distribution obtained at 0.46 ms with lower [F], [R], and P as the one closer to the nascent distribution. Not surprisingly, the surprisal analysis of this distribution led to a nonlinear plot (correlation coefficient 0.7), and so we assumed the ratio of P_0/P_1 to be 3 (close to the P_1/P_2 ratio). The distribution obtained is P_0-P_4 = 67:22:8:2:1, and the lower limit for $\langle f_v(HCl)\rangle$ is 0.06. For comparison, assuming P_0/P_1 to be 2 leads to $\langle f_v(HCl)\rangle$ of 0.07.

The energy disposal from elimination reactions has been treated in detail by Zamir and Levine.[28] The vibrational energy

appearing in the HX product has contributions from the excess energy, E_x, above the threshold energy and from the potential energy, E_p, which is basically the barrier for the reverse addition reaction. i.e.,

$$E_v(\mathrm{HX}) = aE_x + bE_p \qquad (2)$$

This sum rule was used to interpret the energy disposal from HX elimination reactions of haloethanes.[5,13,14] The *b* values estimated were typically 0.24−0.3 for four-centered reactions. For the HCl elimination from CH_3COCl, the barrier energy, $E°$, is 48.9 kcal mol^{-1} (vide infra). From section III.a., E_{av} = 85 kcal mol^{-1} and $\Delta H°(0\ \mathrm{K}) = 19.9$ kcal mol^{-1}. This implies that $E_p = E° - \Delta H° = 28.3$ and $E_x = E_{av} - E_p = 56.7$ kcal mol^{-1}. The "*a*" parameter in the above equation can be estimated using the transition state frequencies,[10] and the method is described in detail in ref 5. For this reaction $a = 0.05$, and it is typical for the four-centered elimination reactions.[5] Using this "*a*" in eq 2, the "*b*" is calculated to be 0.247, which is almost identical to that for HF elimination from CH_3CH_2F and CF_3CH_3.[5] This shows that the dynamics of HCl formation from H + CH_2COCl is very similar to that of the HX elimination from haloethanes, i.e., HCl is formed from the vibrationally excited CH_3COCl and not by direct abstraction of Cl from CH_2-COCl by H. It should be pointed out that the H + CH_2CH_2Cl reaction, under very similar conditions, led to an inverted distribution of HCl(v) that would be expected for a Cl abstraction mechanism.[29] Also, recently Leone and co-workers have studied the O + CH_3CH_2 reaction and observed inverted OH(v) distribution, explaining it in terms of a direct H abstraction mechanism.[30]

The *a* and *b* values obtained above for CH_3COCl can be used to predict the nascent $\langle f_v(\mathrm{HCl})\rangle$ for the HCl elimination from FCH_2COCl. The threshold energy for HCl elimination is calculated to be 60.7 kcal mol^{-1} (vide infra). For a C−F bond energy of 108 and thermal energy of CH_2COCl (3.1), $E_x = 51$ and $E_p = 22$, all in kcal mol^{-1}. Using the sum rule, eq 2, gives $\langle f_v\rangle = 0.11$ compared to our lower limit of 0.06. Clearly, the observed HCl(v) distribution has been affected by relaxation, and we prefer this estimate of $\langle f_v(\mathrm{HCl})\rangle$ for the HCl elimination from FCH_2COCl. However, the fact that HCl emission was observed from the F + CH_2COCl reaction clearly demonstrates that the reaction goes through vibrationally excited FCH_2COCl*.

e. CO(v = 1 → 0) Emission. In all the FCH_2COCl experiments that produced HCl(v) emission, the CO emission could also be observed. Since only $v = 1 \rightarrow 0$ emission was observed, there is no way of estimating the CO(v = 0) population from our experiments and hence the total CO produced. However, the relative [CO(v = 1)] was estimated by measuring the area under the broad emission spectrum and comparing it to the HCl(v) emission intensity. The [CO(v = 1)] was only 2−7% compared to [HCl(v > 0)], and clearly it is produced in a minor channel. Quantum chemical and RRKM calculations were done to identify the mechanism of CO formation, and these are described next.

IV. Ab Initio Calculations

All calculations were performed using the Gaussian 92 program.[31] All possible reaction pathways were considered for FCH_2COCl in line with the earlier work on CH_3COCl.[10] Optimization of the geometries of the reactants and transition states were carried out at MP2 level using the conventional 6-31G* basis set. All electrons were included for the calculation of correlation energy. Harmonic vibrational frequencies were calculated at the same level to characterize the nature of the stationary points on the potential energy surface. We look at the HCl elimination from CH_3COCl in more detail compared to ref 10 and our calculations for FCH_2COCl reported here, for reasons described below.

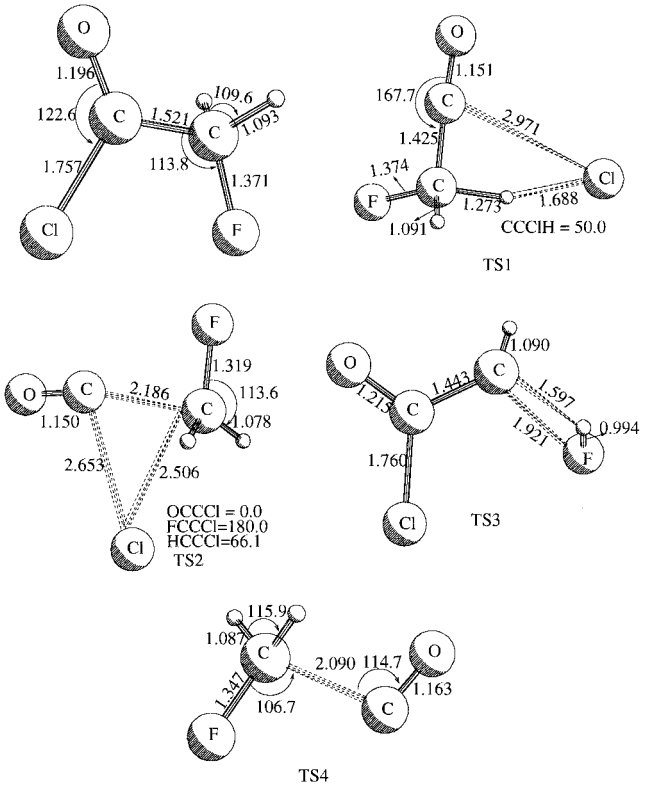

Figure 2. Optimized geometries (MP2/6-31G*) for FCH_2COCl and the transition states for 1,2-HCl elimination (TS1), CO elimination (TS2), 2,2-HF elimination (TS3) and the transition state for $CH_2FCO \rightarrow CH_2F + CO$ (TS4). Distances are given in angstroms and the angles in degrees.

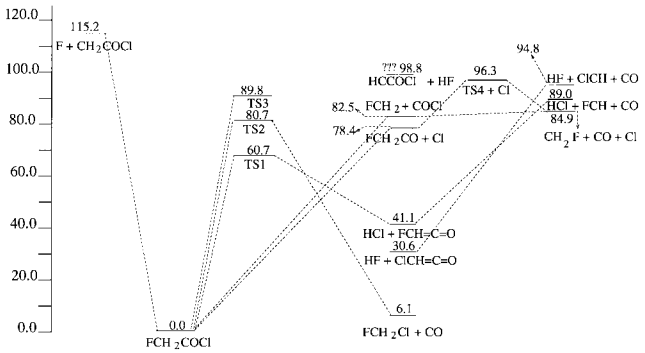

Figure 3. Schematic energy level diagram for the unimolecular reactions of the chemically activated FCH_2COCl (energies in kcal mol^{-1}).

The optimized structures of the various transition states and the reactant, FCH_2COCl, are shown in Figure 2. (The TS geometries for CH_3COCl are given in ref 10, Figure 2, at the HF/6-31G* level.) The bond lengths and bond angles are given in angstroms and degrees, respectively. All the products were optimized at the same level for thermochemical calculations. Figure 3 graphically summarizes the major conclusions of this work. The zero-point vibrational energy corrected enthalpies of reaction and activation barriers are given in Table 5, along with the estimated enthalpies of reaction given in the previous section. The differences between the two values are ≤7 kcal mol^{-1}, which is expected on the basis of the discussion in section III.a. Experimental results are not available for the barrier

TABLE 5: Thermochemistry for the Unimolecular Reaction Pathways of FCH_2COCl[a]

products	$\Delta H°$(t)	$\Delta H°$(e)	$E°$
$F + CH_2COCl$	115.2	108	115.2
$HCl + CHFCO$	41.1	39	60.7
$CH_2F + COCl$	82.5	83	82.5
$CH_2FCO + Cl$	78.4	83	78.4
$CH_2FCl + CO$	6.1	8	81.0
$CH_2CO + FCl$	76.8	70	>120
$HF + HCCOCl$	98.9?		89.8
$FCHCO \rightarrow CHF + CO$	47.9	42	47.9
$CH_2FCO \rightarrow CH_2F + CO$	6.6	7	17.9
$COCl \rightarrow CO + Cl$	2.4	7	2.4

[a] $\Delta H°$(t) = zero-point vibrational energy corrected enthalpies of reaction calculated at the MP2 level with the 6-31G* basis set in kcal mol^{-1}. $\Delta H°$(e) = enthalpies of reaction estimated using experimental and/or theoretical enthalpies of formation from the literature (see section III.a). $E°$= zero-point vibrational energy corrected threshold energies calculated at the MP2 level with the 6-31G* basis set.

TABLE 6: Unscaled Harmonic Vibrational Frequencies of CH_3COCl, FCH_2COCl, and the Transition States TS1, TS2, TS3, and TS5 (for HCl Elimination from CH_3COCl) at the MP2/6-31G* Level

CH_3COCl	FCH_2COCl	TS1	TS2	TS3	TS5
146.1	113.9	1098.2i	595.5i	609.3i	579.7i
355.8	234.9	120.5	54.3	103.4	79.7
453.2	369.9	163.2	161.6	152.4	177.1
526.4	453.2	219.9	162.1	253.8	317.8
624.6	488.8	304.4	180.0	430.6	411.5
1000.3	787.8	442.5	334.9	472.5	863.3
1085.3	1013.2	626.9	370.1	475.1	1011.7
1161.3	1052.1	865.5	708.3	591.5	1091.3
1450.1	1161.1	1017.4	937.5	700.9	1284.3
1526.9	1286.9	1154.8	1250.1	948.4	1403.9
1528.5	1448.1	1330.5	1267.9	1083.4	1448.4
1869.1	1542.6	1363.8	1500.4	1242.9	1946.2
3127.3	1880.5	1594.0	2110.4	1757.3	2304.5
3220.5	3125.6	2202.6	3292.0	3089.0	3161.4
3245.9	3190.6	3210.5	3462.9	3233.6	3247.3
		Zero-Point Vibrational Energies (kcal mol^{-1})			
30.5	25.9	20.9	22.6	20.8	26.8

energies for any of these reactions for comparison. For ethyl chloride, however, both experimental and theoretical estimates are available.[1] At the MP2/4-31G level, the calculated value was 4 kcal mol^{-1} higher than the experimental barrier for HCl elimination from CH_3CH_2Cl.[1] We expect the ordering of energy barriers for the different channels to be reliable. The C−F bond energy was calculated as 115 kcal mol^{-1}, and the $F + CH_2COCl$ addition reaction was found to have no barrier. The FCH_2COCl* formed in this reaction has more energy than the unimolecular threshold energies calculated for all reactions except $CH_2CO + FCl$ (Table 5). The unscaled harmonic vibrational frequencies of the reactants and transition states are listed in Table 6. The TS characteristics for all the reactions are described below and compared to that of CH_3COCl and haloethanes where applicable.

a. 1,2-HCl Elimination. The most probable reaction pathway for CH_3COCl/FCH_2COCl is the molecular elimination to give $HCl + CH_2CO/CHFCO$ as has been observed experimentally. It proceeds through a loose transition state, TS1 in Figure 3 for FCH_2COCl. The most striking difference observed in this structure compared to the TS structure reported for the HCl elimination from CH_3COCl at the HF/6-31G* level[10] is in the C−Cl distance. It is 2.953/2.971 Å for CH_3COCl/FCH_2COCl at the MP2/6-31G* level, about 0.4 Å shorter than the value for CH_3COCl at the HF/6-31G* level.[10] This can be compared to the 0.15 Å difference between HF and MP2 results with a 4-31G basis for HCl elimination from ethyl chloride. Thus, adding correlation makes a more significant change in the TS geometry for CH_3COCl than for CH_3CH_2Cl. For CH_3COCl, MP2 level optimizations with larger basis sets were done to see if there would be any significant change in the TS structural parameters with the basis size, beyond 6-31G*. Table 7 gives the bond distances at different levels. It is clear that using a larger basis set does not lead to significant changes in the bond distances compared to adding correlation at a given level, especially in the C−Cl and H−Cl bond distances. At the MP2/6-311G** level, the C−Cl distance goes down to 2.836 Å. Adding the diffuse functions (MP2/6-311++G**) makes little difference, and the C−Cl distance is 2.832 Å. The C−C bond distance shows little variation at different levels of calculation. All the ketene dimensions (C−H, C═O, and C═C), in fact, do not vary significantly.

TABLE 7: Bond Distances for the TS for HCl Elimination from CH_3COCl at Different Levels of Calculations[a]

bond	HF/ 6-31G*	HF/ 6-31G**	MP2/ 6-31G*	MP2/ 6-311G**	MP2/ 6-311++G**
H1−C1	1.209	1.199	1.177	1.175	1.182
H2−C1	1.080	1.082	1.091	1.091	1.091
C2−O	1.106	1.105	1.145	1.133	1.134
C1−C2	1.407	1.411	1.408	1.415	1.411
C2−Cl	3.390	3.285	2.953	2.836	2.832
H1−Cl	1.796	1.813	1.891	1.864	1.849

[a] For definition of the distances, see TS2 in Figure 2. Also see ref 10. H1 is the H combining with Cl to form HCl.

The barrier for HCl elimination from FCH_2COCl, reaction R7, is calculated as 60.7 kcal mol^{-1} at the MP2/6-31G*//MP2/6-31G* level which is 12 kcal mol^{-1} higher than that for CH_3COCl (48.9 kcal mol^{-1}) at the same level. Interestingly, the barrier energy for CH_3COCl is very close to that reported in ref 10 (48.2) at the MP2/6-31G*//HF/6-31G* level. Optimization at the MP2 level has not changed the relative energies significantly, though the TS structure has changed. The difference in barrier energies between CH_3COCl and FCH_2COCl is consistent with the fact that halogen substitution at the β-carbon atom increases the barrier height for HX elimination from the haloethanes.[32−35] For example, the barrier energies for HX elimination from CH_2F-CH_2F and CH_2Cl-CH_2Cl are both 5 kcal mol^{-1} higher than those of CH_3CH_2F and CH_3CH_2Cl, respectively.[32,33] The effect of β- fluorination of CH_3COCl appears more dramatic, and our experimental results give only indirect evidence, vide infra. Direct experimental verification is needed to conclusively prove this effect. The $CHFCO \rightarrow CHF + CO$ reaction has a barrier of 48 kcal mol^{-1} which is equal to the C═C bond energy in CHFCO.

The following subsections discuss the other possible pathways for FCH_2COCl*. Our objective here is to identify the mechanism of CO formation and determine the importance of three-centered HF elimination. In the CH_3COCl experiments, no other emission but from HCl(υ) could be seen and so other pathways were not considered in detail.

b. 1,1 Elimination Giving CO. The 1,1 elimination of $FCH_2COCl \rightarrow FCH_2Cl + CO$ has a barrier of 81 kcal mol^{-1}, about 20 kcal mol^{-1} higher than that of HCl elimination. For CH_3COCl, the barrier for CO elimination is much higher at 100.2 kcal mol^{-1}, 52 kcal mol^{-1} above that of HCl elimination. This reaction proceeds through TS2 which consists of elongated C−C (2.19 Å) and C−Cl (2.65 Å) bonds. Analysis of the eigenvector corresponding to the imaginary frequency (595.6i cm^{-1}) suggests that the reaction vector is C−Cl−C bending. A qualitatively similar transition state has been observed for the

dissociation of formamide to $NH_3 + CO$[36] and for the dissociation of acetaldehyde[37] and acetyl chloride[10] to $CH_4 + CO$ and $CH_3Cl + CO$, respectively. The C═O distance is 1.15 Å in TS2 and is identical to the equilibrium value for CO at this level of calculation. This and the fact that the reaction coordinate is C−Cl−C bending imply that CO, if formed from this process, will most likely be in its ground vibrational state.

c. 2,2-HF Elimination. The 2,2-HF elimination from FCH_2COCl leads to the unstable carbene HCCOCl via TS3. It has a barrier of 90 kcal mol^{-1}, about 42 kcal mol^{-1} higher than that for the 1,2-HCl elimination reaction. The eigenvector corresponding to the imaginary frequency is a combination of C−H and C−F stretches and ∠FCH bending, clearly identifying the TS as corresponding to HF elimination reaction. However, problems were encountered while obtaining the minimum energy structure of the singlet carbene. It is evident from the enthalpy of reaction in Table 5, which is larger than the barrier! Optimization gives rise to a first-order saddle point instead of a minimum. All our attempts to minimize this structure with respect to the negative force constant were proved futile. Clearly, our estimate for $\Delta H°$ for this reaction is not reliable, and hence Figure 3 and Table 5 have a question mark at this limit. It may be that the triplet carbene is closer to the singlet in energy and advanced treatment (MCSCF or MRCI) is required. Detailed study on this carbene is beyond the scope of this work.

d. Bond Dissociation Reactions. The C−C and C−Cl bond dissociation processes were found to be direct dissociation processes with no distinct barrier. Thus, TS structures could not be assigned. The C−Cl bond energy is 78 kcal mol^{-1} and the C−C bond energy is 82 kcal mol^{-1}. This is similar to the result for CH_3COCl where these bond energies were 81 and 87 kcal mol^{-1}, respectively.[10] For CH_3COCl, these values agree closely with the recent estimates[38] of 83 and 86 kcal mol^{-1} based on experimental enthalpies of formation.

The successive fission from CH_3-CO/FCH_2-CO and CO−Cl radicals can lead to CO formation. However, both C−C fission reactions have significant barriers. The C−C bond fission in FCH_2CO radical has a barrier height of 18 kcal mol^{-1}, and it proceeds through transition state TS4. This is comparable to CH_3CO and CF_3CO for which the barrier for C−C bond fission has been calculated as 18 and 12 kcal mol^{-1} at MP2/6-31G* level, respectively.[10,39] It is noteworthy that Lee and co-workers[40] have measured the barrier for CH_3CO dissociation to be 17 ± 1 kcal mol^{-1}, in excellent agreement with Sumathi and Chandra's calculations.[10] The C−Cl bond fission from COCl has no distinct TS, and it is only 2.4 kcal mol^{-1} endoergic at this level. The CO formation could be from reactions R10, R11, + R16, R12 + R14, or R7 + R15. We carried out RRKM calculations with the ab initio TS and molecular parameters to determine the importance of the different channels producing CO. Also, the importance of 2,2-HF elimination has to be ascertained to determine if it can account for the increase in HF($v = 1$ and 2) at longer observation time. The results are given next.

V. RRKM Calculations

The microcanonical rate constant for a given reaction was calculated as

$$k(E) = \frac{I^{\#}}{\hbar}\left(\frac{I^{\#}}{I}\right)^{1/2}\frac{G^{\#}(E - E°)}{N(E)} \qquad (3)$$

The sum of states for the TS, $G^{\#}(E - E°)$, and the density of states for the reactant, $N(E)$, were calculated by direct counting up to 30 kcal mol^{-1} and by Haarhoff approximation for higher energies.[32] For either method, the vibrational frequencies of the molecule/TS (Table 6) were grouped in to seven different values by taking geometric averages with appropriate degeneracies. The moments of inertia for the molecule (I) and the TS ($I^{\#}$) were taken from our ab initio calculations. The reaction path degeneracy $I^{\#}$ depends on the model for each reaction, and $\hbar$ is the Planck's constant.

For HCl elimination from CH_3COCl, TS and molecular parameters were available at HF/6-31G* and MP2/6-31G* levels. Both were used in a TST calculation to estimate the preexponential factor for unit reaction path degeneracy at 800 K. The log A thus calculated was 13.67 and 13.99 at the HF and MP2 levels, respectively. Scaling the HF frequencies uniformally by 0.89 for both TS and molecule did not result in any significant difference, the log A coming out to be almost identical. Both values are larger than the typical experimental value of about 13 for four-centered HCl elimination of haloethanes, e.g., CH_3CH_2Cl (13.08),[41] CH_3CCl_3 (13.15),[3] CH_3CF_2Cl (12.85),[34] and CH_2ClCF_2Cl (12.0).[42] Experimental data for CH_3COCl is not available to the best of our knowledge, and we prefer to use the HF frequencies for the TST and RRKM calculations. It should be pointed out that the TS structure is tighter at the MP2 level compared to that at the HF level. However, the MP2 results for the low-frequency vibrations are too low even when compared to the scaled HF frequencies. The three lowest frequencies for the TS are 79.8, 177.1, and 317.8 at the MP2 level compared to the unscaled HF frequencies 126.7, 293.4, and 414.4 cm^{-1}. For the molecule this is not the case, and hence the preexponential factor increases significantly. Obviously scaling the MP2 frequencies would not improve the situation, unless one uses scaling factors above 1 for the low-frequency vibrations of the TS. For FCH_2COCl, frequency calculations were done only at the MP2 level, and hence the RRKM rate constants for the individual reactions may be upper limits. However, in this case we compare MP2 results for all the reactions, and hence the relative values are expected to be more reliable.

For the bond dissociation reactions R11 and R12, a TS was not found and we modeled the transition states following earlier work on similar systems. For reaction R12 the TS frequencies are estimated by combining the two products' frequencies (CH_2F and COCl) and adding two low-frequency doubly degenerate bending modes (110, 70 cm^{-1}) plus internal rotation, treated here as another low-frequency (55 cm^{-1}) torsion. The ratio of moments of inertia was chosen as 2.45. This led to a preexponential factor, A, of 1.86×10^{16} s^{-1} and log $A = 16.27$ which is comparable to several C−C bond dissociation reactions. For reaction R11, we added two low-frequency bending modes to that of FCH_2CO (70 cm^{-1}), and the moments of inertia ratio was chosen to be 2.66. We followed the model developed by Rakestraw and Holmes for CF_3CH_2Cl.[35] The log A for this TS was 14.62, and it is comparable to that of CF_3CH_2Cl (14.6)[35] and CF_3CHFCl (14.7).[43] For CH_3COCl, transition states for C−C and C−Cl dissociation were chosen in a similar fashion. For C−C dissociation, the five frequencies added to those of CH_3 and COCl were 180(2), 130(2), and 80 and log A was 16.02. For C−Cl, the doubly degenerate bending mode frequency was 110 and log A was 14.6. For both these reactions, the recent estimates of bond energies[38] were used as threshold energies in the calculations.

The C−F bond energy in FCH_2COCl is not known other than by our calculations, which gave 115, and our estimate, which was 108 kcal mol^{-1}. The thermal energy for CH_2COCl at 300

TABLE 8: RRKM Rate Constants for Unimolecular Reactions of FCH_2COCl^*/CH_3COCl^a

	105		110		115	
reaction	*k*	%	*k*	%	*k*	%
HCl + CHFCO (13.93)	7.45E11[b]	74.1	1.28E11	59.6	2.07E11	46.4
CH_2F + COCl (16.27)	2.40E10	23.9	8.07E10	37.6	2.24E11	50.3
CH_2FCO + Cl (14.62)	1.15E09	1.1	3.45E9	1.6	7.59E09	1.7
CH_2FCl + CO (14.79)	8.83E08	0.9	2.71E09	1.3	6.96E09	1.6
CHCOCl + HF (13.96)	6.28E06		3.46E07		1.36E08	
CH_2CO + HCl (13.67)	4.03E11	98.2	5.66E11	95.1	7.68E11	89.5
CH_3 + COCl (16.01)	6.79E09	1.7	2.75E10	4.7	8.65E10	10.2
CH_3CO + Cl (14.62)	3.66E08	0.1	1.06E09	0.2	2.60E09	0.3

[a] Column titles give the energy of the molecule in kcal mol^{-1}, *k* is the RRKM rate constant in s^{-1}, given in scientific notation, and % is the percentage contribution of the given reaction to the total rate constant at this energy. The number in parentheses next to the products gives log *A*, the logarithm of the preexponential factor at 800 K calculated using transition state theory per unit reaction path degeneracy. Reaction path degeneracy is 2 for HCl and HF elimination and 1 for all other reactions. The last three lines are for CH_3COCl. [b] Read as 7.45×10^{11}.

K is 3.1 kcal mol^{-1}, and it should be added to the C−F bond energy to obtain the average energy, $\langle E \rangle$, of the FCH_2COCl^* produced. For FCH_2COCl, the $\langle E \rangle$ should be between 110 and 115 kcal mol^{-1} in our experiments. For CH_3COCl, the $\langle E \rangle$ in our experiments is estimated as 105 kcal mol^{-1} from the C−H bond energy. Table 8 gives the calculated rate constants for five different channels from FCH_2COCl and three channels for CH_3COCl. The percent contributions for each channel to the total reaction at $\langle E \rangle = 105$, 110, and 115 kcal mol^{-1} are also included. The first column is applicable to CH_3COCl, and the other two are representative results for FCH_2COCl.

Clearly, HCl elimination is the important channel for both molecules at these energies. The C−C dissociation is equally important for FCH_2COCl but not for CH_3COCl. The critical factors are certainly the differences in the threshold energy between HCl elimination and C−C dissociation and $\langle E \rangle$ for the two cases. For FCH_2COCl, the difference is 22, but for CH_3COCl it is 38 kcal mol^{-1}. The C−Cl dissociation channel does not contribute significantly even though the critical energy for it is 3−4 kcal mol^{-1} less than that of C−C dissociation. The larger preexponential factor for C−C dissociation, compared to that of C−Cl ($\log A = 16.2$ vs 14.6), dominates the reaction rates. For FCH_2COCl, the CO elimination contributes ≈1% to the total reaction and the HF elimination reaction is not important at all.

The above results clearly indicate that the CO formation from FCH_2COCl is mainly through C−C dissociation followed by $COCl \rightarrow CO + Cl$. The later reaction has a very small barrier (7 kcal mol^{-1}) which supports our expectation. The C−Cl dissociation is less important and the $FCH_2CO \rightarrow FCH_2 + CO$ reaction also has a larger barrier (18 kcal mol^{-1}), virtually eliminating reactions R10 + R16 as a possible source for CO. The $CHFCO \rightarrow CHF + CO$ reaction has a large barrier of 48 kcal mol^{-1}. The HCl + CHFCO products have available energy of 72 kcal mol^{-1}. At least 67% of this energy has to remain in CHFCO for this channel to be allowed. The 1,2-HF elimination from CF_3CH_3 and CH_3CH_2F lead to 60% of the available energy as olefin's internal energy.[5] It is clear that the $CHFCO \rightarrow CHF + CO$ does not significantly contribute to CO formation in our system.

The RRKM results on CH_3COCl give a reasonable explanation for our not observing any CO emission in the experiments along with HCl emission. (Of course, our experiments cannot rule out CO formation in the ground vibrational state.) The C−C dissociation contributes less than 2% to the total reaction at 105 kcal mol^{-1} energy. These results are also important in the context of recent photodissociation experiments on CH_3COCl.[40,44,45] These experiments have clearly demonstrated that the photodissociation is impulsive, occurring on a subpicosecond time scale leading exclusively to C−Cl dissociation. Thus it does not follow the usual Norrish type I mechanism for aldehydes and ketones which predicts the cleavage of the weaker α bond to that of the carbonyl group following internal conversion to the ground state. Our calculations show that if the Norrish type I mechanism is followed, one would expect to see C−C dissociation rather than C−Cl dissociation. However, C−C dissociation is important not because it is the weaker bond in a traditional sense but because of the entropy effects leading to a larger preexponential factor compared to that for C−Cl dissociation. Thus, if the α bond energies are not too different as in this case, the entropy factors should favor the dissociation into two polyatomic fragments rather than to an atom + a polyatomic fragment.

After completion of this work, we came across the recent paper by Maricq et al.[46] on the diode laser study of the Cl + CH_3CO reaction. They observed the HCl + CH_2CO channel only. From their experiments they could not differentiate between addition−elimination mechanism (CH_3COCl formation followed by HCl elimination) and direct abstraction of H by Cl from CH_3CO. Two of their observations need to be considered. (1) There is no pressure dependence on the CH_2CO formation rate constant in the range 10−200 Torr. (2) The time dependence of the IR absorption profile of CH_2CO did not show any difference when the buffer gas was changed from N_2 to C_2F_6. This was verified to determine if the ketene formed was vibrationally excited, and the conclusion was that ketene product did not have any significant internal excitation.

For the addition−elimination mechanism, if collisional stabilization competes with the unimolecular reaction in the 10−200 Torr pressure range, the ketene formation rate constant should be pressure dependent. From our RRKM calculations, we estimate the rate constant for the HCl + CH_2CO channel at 83 kcal mol^{-1} (the C−Cl bond energy in acetyl chloride) to be 1.0×10^{11} s^{-1}. Only the HCl elimination channel is expected at this energy. The collision frequency in 200 Torr N_2 is about 4×10^9 s^{-1}, assuming $d = 6$ Å for the N_2-CH_3COCl pair. Clearly, the unimolecular reaction rate is much faster and point 1 above is consistent with the addition−elimination mechanism. However, their second observation is somewhat puzzling if this mechanism were to be followed. For HX elimination from haloethanes, 50−60% of the available energy goes to the internal degrees of the alkene product.[5] Our TS structure for HCl elimination from CH_3COCl indicates that the ketene product is not fully formed yet. Hence, one would expect to see vibrational excitation of ketene. However, as the authors point out, their experiment could not rule out excitation in modes that have

little anharmonic coupling with the ν_2 mode they observed. Direct observation of HCl(v) and CH_2CO internal energy distributions are needed for definitive answers.

VI. Conclusions

Infrared chemiluminescence from a flow reactor has been used to study the F + CH_3COCl and H + ICH_2COCl reaction systems. The primary reaction in the former system leads to an inverted HF(v) distribution of $P_1-P_3 = 21:52:27$. From the highest observed HF(v, J) product state, the C−H bond energy in CH_3COCl is estimated as $\leq$101.2 kcal mol^{-1}. A linear surprisal analysis using model 2 prior gives the complete distribution as $P_0-P_3 = 3:20:50:27$ with $\langle f_v \rangle = 0.6$, which is typical for H abstraction by F from polyatomic molecules. From the secondary F + CH_2COCl reaction, HCl(v) and CO(v) emissions were observed, the latter being less than 10% of the former. The HCl(v) distribution, which was partially relaxed, was estimated as $P_0-P_4 = 67:22:8:2:1$ with $\langle f_v \rangle = 0.06$. The H + CH_2COCl reaction resulted in only HCl(v) emission, and the nascent vibrational distribution was $P_0-P_4 = 36.4:24.9:20.3:12.4:6.0$. The $\langle f_v \rangle$ was 0.12, and it was comparable to that from unimolecular elimination reactions from haloethanes.

Quantum chemical ab initio calculations were carried out at the MP2 level with the 6-31G* basis set to determine the threshold energies for various reaction pathways for the energized FCH_2COCl^* formed by the F + CH_2COCl reaction. The HCl elimination from CH_3COCl was studied at the MP2 level with larger basis sets up to 6-311++G**. The ab initio TS geometries for HCl elimination from both these molecules are loose, leading to large preexponential factors in TST calculations. Increasing the basis set to 6-311++G** did not make any significant difference in the TS structure for CH_3COCl. Our results are similar to that of ethyl chloride reported in ref 1. These results do not agree with the available experimental preexponential factors for ethyl chloride.[41] For CH_3COCl, experimental results are not available yet.

For FCH_2COCl, the 1,2-HCl elimination channel leading to HCl + CHFCO was found to have the smallest barrier of 60 kcal mol^{-1}. RRKM calculations indicate that the HCl elimination channel dominates the unimolecular reactions at $\langle E \rangle \leq 105$ kcal mol^{-1}. The CO formation occurs through successive bond dissociation i.e., CH_2F + COCl followed by COCl → CO + Cl. For both these molecules, although the C−Cl bond energy is calculated to be smaller than the C−C bond energy, the C−Cl dissociation rate is slower than that of C−C dissociation due to entropy factors.

Acknowledgment. R.S. thanks the Alexander van Humboldt Stiffung for financial support. The experimental work at Kansas State University was supported by NSF Grant No: 9505032. We thank the anonymous referees for some useful comments.

References and Notes

(1) Toto, J. L.; Pritchard, G. O.; Kirtman, B. *J. Phys. Chem.* **1994**, *98*, 8359.
(2) Clough, P. N.; Polanyi, J. C.; Taguchi, R. T. *Can. J. Chem.* **1970**, *48*, 2919.
(3) Sudbo, Aa. S.; Schulz, P. A.; Shen, Y. R.; Lee, Y. T. *J. Chem. Phys.* **1978**, *69*, 2312.
(4) Quick C. R.; Wittig, C. *J. Chem. Phys.* **1980**, *72*, 1694.
(5) Arunan, E.; Wategaonkar, S. J.; Setser, D. W. *J. Phys. Chem.* **1991**, *95*, 1539.
(6) Seakins, P. W.; Woodbridge, E. L.; Leone, S. R. *J. Phys. Chem.* **1993**, *97*, 5633.
(7) Kato S.; Morokuma, K. *J. Chem. Phys.* **1980**, *73*, 3900.
(8) Benito, R. M.; Santamaria, J. *J. Phys. Chem.* **1988**, *92*, 5028.
(9) Raff, L. M.; Graham, R. W. *J. Phys. Chem.* **1988**, *92*, 5111.
(10) Sumathi, R.; Chandra, A. K. *Chem. Phys.* **1994**, *181*, 73.
(11) Holmes, B. E.; Setser, D. W. In *Physical Chemistry of fast reactions*; Smith, I. W. M., Ed.; Plenum: New York, 1980; Vol. 2.
(12) Agrawalla, B. S.; Setser, D. W. In *Gas-Phase Chemiluminescence and Chemiionization*; Fontijn, A., Ed.; Elsevier: Amsterdam, 1985.
(13) Butkovskaya, N. I.; Zhao, Y.; Setser, D. W. *J. Phys. Chem.* **1994**, *98*, 10779.
(14) Butkovskaya, N. I.; Manke, G., II; Setser, D. W. *J. Phys. Chem.* **1995**, *99*, 11115.
(15) Xu, S.; Beran, K. A.; Harmony, M. D. *J. Phys. Chem.* **1994**, *98*, 2742.
(16) Arunan, E.; Setser, D. W.; Ogilvie, J. F. *J. Chem. Phys.* **1992**, *97*, 1734.
(17) Langhoff, S. R.; Bauschlicher, C. W., Jr. *J. Chem. Phys.* **1995**, *102*, 5220.
(18) McMillen, D. F.; Golden, D. M. *Annu. Rev. Phys. Chem.* **1982**, *33*, 493.
(19) Chase, M. W., Jr.; Davies, C. A.; Downey, J. R., Jr.; Frurip, D. J.; McDonald, R. A.; Syverud, A. N. *J. Phys. Chem. Ref. Data.* **1985**, *14* (Suppl. No. 1). Wagman, D. D.; Evans, W. H.; Parker, V. B.; Schumm, R. H.; Halow, J.; Bailey, S. M.; Churney, K. C.; Nuttal, R. L. *J. Phys. Chem. Ref. Data*. **1982**, *11* (Suppl. No. 2).
(20) ΔH°_f(0 K) from ab initio calculations of Wiberg, K. B.; Hadad, C. M.; Rablen, P. R.; Cioslowski, J. *J. Am. Chem. Soc.* **1992**, *114*, 8644. These authors quote experimental ΔH°_f (298 K) of −58.0 ± 0.2 from Pedley, J. B.; Naylor, R. D.; Kirby, S. P. *Thermochemical Data of Organic Compounds*, 2nd ed.; Chapmann and Hall: London, 1986.
(21) Nicovich, J. M.; Kreutter, K. D.; Wine, P. H. *J. Phys. Chem.* **1990**, *92*, 3539.
(22) Nuttal, R. L.; Laufer, A. H.; Kilday, M. V. *J. Chem. Thermodyn.* **1971**, *3*, 167.
(23) Lias, S. G.; Karpas, Z.; Liebman, J. F. *J. Am. Chem. Soc.* **1985**, *107*, 6089.
(24) Pritchard, G. O.; Nilsson, W. B.; Kirtman, B. *Int. J. Chem. Kinet.* **1984**, *16*, 1637.
(25) Rodriquez, C. F.; Hopkinson, A. C. *J. Phys. Chem.* **1993**, *97*, 849. Note: Very recently, Poutsoma, J. C.; Paulino, J. A.; Squires, R. R. *J. Phys. Chem. A* **1997**, *101*, 5327 have recommended ΔH°_f(298 K) for CHF as 34.2 kcal mol^{-1}, nearly identical to the value we have used.
(26) Zachariah, M. R.; Westmoreland, P. R.; Burgess, D. R., Jr.; Tsang, W.; Melius, C. F. *J. Phys. Chem.* **1996**, *100*, 8737.
(27) Arunan, E.; Raybone, D.; Setser, D. W. *J. Chem. Phys.* **1992**, *97*, 6348.
(28) Zamir, E.; Levine, R. D. *Chem. Phys.* **1980**, *52*, 253.
(29) Arunan, E.; Rengarajan, R.; Setser, D. W. *Can. J. Chem.* **1994**, *72*, 568.
(30) Lindner, J.; Loomis, R. A.; Klaassen, J. J.; Leone, S. R. *J. Chem. Phys.* **1998**, *108*, 1944.
(31) Frisch, M. J.; Trucks, G. W.; Head-Gordon, M.; Gill, P. M. W.; Wong, M. W.; Foresman, J. B.; Johnson, B. G.; Schlegel, H. B.; Robb, M. A.; Replogle, E. S.; Gomperts, R.; Andres, J. L.; Ragavachari, K.; Binkley, J. S.; Gonzalez, C.; Martin, R. L.; Fox, D. J.; Defrees, D. J.; Baker, J.; Stewart, J. J. P.; Pople, J. A. *Gaussian 92, Revision C*; Gaussian Inc.: Pittsburgh, PA, 1992.
(32) Robinson, P. J.; Holbrook, K. A. *Unimolecular Reactions*; Wiley: New York, 1972.
(33) Forst, W. *Theory of Unimolecular Reactions*; Academic Press: New York, 1973.
(34) Jones, Y.; Holmes, B. E.; Duke, D. W.; Tipton, D. L. *J. Phys. Chem.* **1990**, *94*, 4957.
(35) Rakestraw D. J.; Holmes, B. E. *J. Phys. Chem.* **1991**, *95*, 3968.
(36) Takumoto, T.; Saito, S.; Imamura, A. *J. Phys. Chem.* **1985**, *89*, 2286.
(37) Yadav, J. S.; Goddard, J. D. *J. Chem. Phys.* **1986**, *84*, 2682.
(38) Arunan, E. *J. Phys. Chem. A* **1997**, *101*, 4838.
(39) Marciq, M. M.; Szente, J. J.; Khitrov, G. A.; Dibble, T. S.; Fransisco, J. S. *J. Phys. Chem.* **1995**, *99*, 11875.
(40) North, S.; Blank, D. A.; Lee, Y. T. *Chem. Phys. Lett.* **1994**, *224*, 38.
(41) Dees, K.; Setser, D. W. *J. Chem. Phys.* **1968**, *49*, 1193.
(42) Ishikawa, Y.; Arai, S. *Bull. Chem. Soc. Jpn.* **1994**, *57*, 681.
(43) Yokoyama, A.; Yokoyama, K.; Fujisawa, G. *J. Chem. Phys.* **1994**, *100*, 6487.
(44) Person, M. D.; Kash, P. W.; Butler, L. J. *J. Chem. Phys.* **1992**, *97*, 355.
(45) Deshmukh, S.; Hess, W. P. *J. Chem. Phys.* **1994**, *100*, 6429.
(46) Maricq, M. M.; Ball, I. C.; Straccia, A. M.; Szente, J. J. *Int. J. Chem. Kinet.* **1997**, *29*, 421.